Journal of Theoretical and Applied Mechanics, Sofia, 2012, vol. 42, No. 1, pp. 23–40

SOLID MECHANICS

CALCULATION OF STRESS INTENSITY FACTORS BASED ON FORCE-DISPLACEMENT CURVE USING ELEMENT FREE GALERKIN METHOD*

Sonia Parvanova
University of Architecture, Civil Engineering and Geodesy,
1, Christo Smirnenski Blvd, 1046, Sofia, Bulgaria,
e-mail: slp_fce@uacg.bg

[Received 26 August 2011. Accepted 27 February 2012]

Abstract. An idea related to the calculation of stress intensity factors based on the standard appearance of the force-displacement curve is developed in this paper. The presented procedure predicts the shape of the graphics around the point under consideration form where indirectly the stress intensity factors are obtained. The numerical implementation of the new approach is achieved by using element free Galerkin method, which is a variant of meshless methods and requires only nodal data for a domain discretization without a finite element mesh. A MATLAB software code for two dimensional elasticity problems has been worked out, along with intrinsic basis enrichment for precise modelling of the singular stress field around the crack tip. One numerical example of a rectangular plate with different lengths of a symmetric edge crack is portrayed. The stress intensity factors obtained by the present numerical approach are compared with analytical solutions. The errors in the stress intensity factors for opening fracture mode I are less than 1% although the model mesh is relatively coarse.
Key words: Element free Galerkin method, two dimensional elasticity problems, Fracture mechanic, Stress intensity factors.

1. Introduction

The effective and accurate calculation of Stress Intensity Factors (SIF) is one of the basic problems in Linear Elastic Fracture Mechanics (LEFM) [1] [2]. Two principal approaches are known for a SIF calculation: local, based

*The financial support of project BG051PO001–3.3.05.–0001 "Science and business", funded on Operational program "Development of human resources" at the "European social fund" is highly appreciated.

on the use of displacements or tractions near to the crack tip; and global or energy methods, which are based on the calculation of the energy release rate in terms of crack growing. Both methods possess a number of variants with respective pros and cons and many various SIF solutions are now available in the literature. The local methods are based on the use of the first term, which is the required SIF, on the infinite series expansion of the William's solution [3], worked out for an elastic body with pre-existing crack. In that case, the displacements of the stress free crack faces can be used, as well as the stresses of the continuum in the vicinity of the crack tip. The disadvantage of the local methods is that the parameters used (tractions or displacements) are loaded with error due to their nearness to the singular point. In that case, special singular quarter points finite or boundary elements should be used in order to represent properly the stress singularity at the crack tip, which implies the use of special purpose software programs. Any commercial numerical method codes cannot be properly used for the local methods.

Contrary to the local methods, the energy methods use quantities which are located far away from the singular point. That leads to the derivation of relatively accurate results with a rather coarse mesh of elements. The calculation of the energy release rate and the path independent J-integral method are the most widely used approaches among the energy methods. The difficulties with decomposition of energy release rate in case of mixed mode crack propagation are associated with energy methods. That is considered as a disadvantage of the energy methods although several techniques have been developed for such decomposition [4].

Different numerical methods could be used for modelling of the crack problems, such as the most universal finite element method (FEM), boundary element method (BEM) or mesh-less methods. The problem arises with modelling of the crack tip region, even when a very fine mesh is used, because of the singular stress field around the crack tip. Meshless methods in computational mechanics have been widely developed in recent decades. The main difference between meshless methods and conventional numerical methods is the way of shape function formation. The meshless method follows the same procedure once the shape function has been obtained to form equations and get a solution of the problem as the other numerical methods. These methods are very suitable for fracture mechanics problems because in case of crack propagation no remeshing is needed with the new crack increment, just additional nodes around the crack tip should be introduced.

In the present paper, Element Free Galerkin (EFG) method is used to develop one new idea related to the accurate derivation of the SIF for pure

opening mode I of fracture. That idea is based on the standard appearance of the force-displacement curve in LEFM. In a relatively simple manner, the shape of the latter curve is caught wherefrom indirectly the SIF, respectively energy release rate, could be easily obtained. The advantage of the proposed technique is that the fracture parameters could be easily and quite accurate derived by using any commercial numerical method codes with relatively coarse model mesh.

The EFG method is a kind of meshless methods given in detail in a number of papers of Belitchko and al. as well as of Liu and al. [7]–[11]. A MATLAB software code, for two dimensional elasticity problems, has been developed based on theory described below as well as on the MATLAB source programs given in the paper [9]. One numerical example is portrayed and the relevant results are obtained using the latter code. The SIFs calculated for different crack lengths and different numerical models are compared with analytical solutions given in the literature.

2. Formulation of the element free Galerkin method

Element free Galerkin method is a mesh-less method, as far as no finite elements are needed to establish connectivity between different nodes. The EFG method uses Moving Least Squares (MLS) technique, with variable coefficients, to approximate the function $u(\mathbf{x})$ with $u^h(\mathbf{x})$ at an arbitrary point with coordinates $\mathbf{x}^T = \{x, y\}$ of the domain under consideration [9]. The MLS method consists of three basic components: a weight function, $w(\mathbf{x} - \mathbf{x}_i)$, defined in a compact support around each node of the model; a basis, which is usually a polynomial of a definite order; and a set of non-constant coefficients, $a_i(x, y)$, which depends on the point under consideration. The weight function is nonzero over a small sub-domain around a node of the model and this sub-domain is called node's support. The latter is also known as a domain of influence. The overlap of the nodal domains of influence ensures the nodal connectivity [6]–[10].

The continuity of the MLS approximants depends on the continuity of the weight function. With other words a low order polynomial basis (for example linear) could be used to generate highly continuous approximants by choosing an appropriate weight function [9].

2.1. Approximation by MLS method

Each node of the model has so called "nodal parameter" $u_i(\mathbf{x})$, which has influence on the displacement function $u(\mathbf{x})$ at the same node, but in general both functions $u_i(\mathbf{x})$ and $u(\mathbf{x})$ are different. The field variable $u(\mathbf{x})$ (a

component of the displacement) of any point within the problem domain with coordinates (x, y) is approximated applying MLS method as follows:

$$u^h(\mathbf{x}) = \sum_{j=1}^{m} p_j(\mathbf{x}) \cdot a_j(\mathbf{x}) = \mathbf{p}^{\mathrm{T}}(\mathbf{x})\, \mathbf{a}(\mathbf{x}). \tag{1}$$

In equation (1) $\mathbf{p}(\mathbf{x})$ is a basis, which is usually a complete polynomial of order m, respectively m is the number of components of the basis; $\mathbf{a}(\mathbf{x})$is a vector of non-constant coefficients. These approximations are known as MLS interpolants in curve and surface fitting and could be found in [5]. Currently such approximation is widely used in mesh-free methods [6]–[10].

The non-constant coefficients $\mathbf{a}(\mathbf{x})$ are determined so as to minimize, with respect to $\mathbf{a}(\mathbf{x})$, the following weighted, discrete L_2 norm:

$$J = \sum_{i=1}^{n} w(\mathbf{x} - \mathbf{x}_i) \left[\mathbf{p}^{\mathrm{T}}(\mathbf{x}_i)\, \mathbf{a}(\mathbf{x}) - u_i\right]^2, \tag{2}$$

where n is the number of nodes belonging to the domain of influence of point $\mathbf{x}$ for which the weight function $w(\mathbf{x} - \mathbf{x}_i) \neq 0$; u_i is the nodal parameter of i-th node at $\mathbf{x} = \mathbf{x}_i$. Substituting the obtained expressions, for non-constant coefficients $\mathbf{a}(\mathbf{x})$, back in equation (1) for the scalar function $u(\mathbf{x})$ is reached:

$$\begin{aligned} u^h(\mathbf{x}) &= \mathbf{p}^{\mathrm{T}}(\mathbf{x})\, \mathbf{A}^{-1}(\mathbf{x})\, \mathbf{B}(\mathbf{x})\, \mathbf{U}_s \\ &= \sum_{i=1}^{n} \sum_{j=1}^{m} p_j(\mathbf{x}) \left(\mathbf{A}^{-1}(\mathbf{x})\, \mathbf{B}(\mathbf{x})\right)_{ji} u_i = \sum_{i=1}^{n} \Phi_i(\mathbf{x})\, u_i, \end{aligned} \tag{3}$$

where $\Phi_i(\mathbf{x})$ is a shape function for the i-th node of the model, $\mathbf{U}_s$is a vector of nodal displacements for nodes within the domain of influence of the point under consideration. Matrices $\mathbf{A}(\mathbf{x})$ and $\mathbf{B}(\mathbf{x})$ are products obtained after the minimization of the discrete L_2 norm and could be found in detail in papers [9] and [10]. The shape function $\Phi_i(\mathbf{x})$, for the i-th node, can be written as:

$$\Phi_i(\mathbf{x}) = \sum_{j=1}^{m} p_j(\mathbf{x}) \left(\mathbf{A}^{-1}(\mathbf{x})\, \mathbf{B}(\mathbf{x})\right)_{ji} = \mathbf{p}^{\mathrm{T}}(\mathbf{x})\, \mathbf{A}^{-1}(\mathbf{x})\, \left(\mathbf{B}(\mathbf{x})\right)_i. \tag{4}$$

It should be pointed out that the EFG shape functions do not satisfy Kronecker delta criterion. That is why, they are called approximants, not interpolants [9]. The approximation of the displacement of the i-th node depends on the nodal parameter u_i as well as on the nodal parameters of all nodes within its domain of influence. This special feature makes the fulfilment of essential boundary conditions more complicated compared with the finite element method. In this paper, the method of Lagrange multipliers is used to enforce the displacement boundary conditions, given in detail in papers [9] and [10].

2.2. Choice of the weight function

The weight function plays an important role concerning the performance of MLS approximation. The weight function must be smooth and positive, having relatively large values in the vicinity of the model nodes and monotonically decreasing for outlying points.

In this paper, the weight function used is taken from paper [9]. The latter is a tensor product weight with cubic spline function. Let the distances r_x and r_y are defined such as $r_x = \|\mathbf{x} - \mathbf{x}_i\| / d_{mx}$ and $r_y = \|\mathbf{x} - \mathbf{x}_i\| / d_{my}$, $d_{mx} = d_{\max} c_{ix}$, $d_{my} = d_{\max} c_{iy}$. The lengths c_{ix} and c_{iy}, concerning the i-th node, are the maximum distances in both directions to the nearest neighbour nodes of the model. The latter ensures that each node has at least two neighbours in both directions within its domain of influence, which is absolutely necessary to guarantee the derivation of non-singular and invertible matrix $\mathbf{A}$ from equations (3) and (4). The value $d_{\max}$ is a scaling parameter which is typically 2.0–4.0 for static analysis. The quantities d_{mx} and d_{my} are the dimensions of the i-th node domain of influence in x and y directions respectively.

The tensor product weight function at any given point is presented by [9]:

$$w(\mathbf{x} - \mathbf{x}_i) = w(r_x) \cdot w(r_y) = w_x \cdot w_y, \tag{5}$$

where the function $w(r)$ is given by the following expression (r could be r_x or r_y respectively):

$$w(r) = \begin{cases} \dfrac{2}{3} - 4r^2 + 4r^3 & \text{for} \quad r \le \dfrac{1}{2} \\ \dfrac{4}{3} - 4r + 4r^2 - \dfrac{4}{3} r^3 & \text{for} \quad \dfrac{1}{2} < r \le 1 \\ 0 & \text{for} \quad r > 1 \end{cases} . \tag{6}$$

The spatial derivatives of the weight function, necessary to compute the spatial derivatives of the shape function, in due form the derivatives of the $\mathbf{A}$ and $\mathbf{B}$ matrices from equations (4), could be found in detail in paper [9].

2.3. Formulation of discrete equations

The standard variational or weak form of equilibrium equation in two dimensions, for EFG method, is given in detail in papers [7], [8], [9], [10]. Consider a trial function $\mathbf{u}(\mathbf{x})$, Lagrange multipliers λ for all test functions

$\delta\mathbf{u}(\mathbf{x})$ and $\delta\lambda$ the standard weak form is [10]:

$$(7)\quad \int_\Omega (\partial\,\delta\mathbf{u})^{\mathrm{T}}\mathbf{D}\,\partial\,\mathbf{u}\,d\Omega - \int_\Omega \delta\mathbf{u}^{\mathrm{T}}\mathbf{b}\,d\Omega - \int_{\Gamma_t} \delta\mathbf{u}^{\mathrm{T}}\bar{\mathbf{t}}\,d\Gamma_t - \int_{\Gamma_u} \delta\lambda^{\mathrm{T}}(\mathbf{u}-\bar{\mathbf{u}})d\Gamma - \int_{\Gamma_u} \delta\mathbf{u}^{\mathrm{T}}\lambda d\Gamma = 0,$$

where ∂ is the matrix differential operator, $\mathbf{D}$ is the matrix of elastic constants, $\mathbf{b}$ is the body force vector, $\mathbf{u}$ is the displacement vector, $\bar{\mathbf{u}}$ is the vector of prescribed displacements on the essential boundaries, $\bar{\mathbf{t}}$ is the prescribed traction vector on the natural boundaries. The last two terms in equation (7) are produced by the method of Lagrange multipliers for fulfilment of the essential boundary conditions in the case when $\mathbf{u}-\bar{\mathbf{u}} \neq 0$. The Lagrange multipliers can be viewed as smart forces that strength $\mathbf{u}-\bar{\mathbf{u}} = 0$ [10].

In order to obtain discretized formulation from the weak form (7), the variations $\mathbf{u}(\mathbf{x})$ and $\delta\mathbf{u}(\mathbf{x})$ should be approximated in accordance with equation (3). The Lagrange multipliers λ need to be interpolated using their nodal values as follows:

$$(8)\qquad \lambda(\mathbf{x}) = N_i(s)\cdot\lambda_i, \quad x\in\Gamma_u; \quad \delta\lambda(\mathbf{x}) = N_i(s)\cdot\delta\lambda_i, \quad x\in\Gamma_u,$$

where $N_i(s)$ is a Lagrange interpolant, s is the arclength along the boundary. $N_i(s)$ is a shape function for the i-th node on the essential boundary. In the present paper, a linear interpolation along the essential boundary is assumed. Finally, discrete equations, obtained by substituting the trial functions, test functions and Lagrange multipliers (8) into the weak form (7), are as follows [9], [10]:

$$(9)\qquad \begin{bmatrix} \mathbf{K} & \mathbf{G} \\ \mathbf{G}^{\mathrm{T}} & 0 \end{bmatrix} \begin{Bmatrix} \mathbf{u} \\ \boldsymbol{\lambda} \end{Bmatrix} = \begin{Bmatrix} \mathbf{f} \\ \mathbf{q} \end{Bmatrix}.$$

In equation (9), $\mathbf{K}$ is the standard global stiffness matrix of dimension $2N\times 2N$ (N is the number of model nodes). $\mathbf{G}$ is the global matrix, of dimension $2N\times N_u$ (N_u is the number of prescribed displacements on the essential boundaries), formed by assembling $\mathbf{G}_{ik}$ (dimension 2×2), defined as:

$$(10)\qquad \mathbf{G}_{ik} = -\int_{\Gamma_u} \Phi_i^{\mathrm{T}}\mathbf{N}_k d\Gamma.$$

A vector that collects the nodal Lagrange multipliers for all nodes on essential boundaries is $\boldsymbol{\lambda}$ in expression (9); $\mathbf{f}$ is the standard global force vector, $\mathbf{q}$ is a global vector of dimension $N_u\times 1$, which is formed by assembling the vectors $\mathbf{q}_k$ for each of the nodes with prescribed displacements:

$$(11)\qquad \mathbf{q}_k = -\int_{\Gamma_u} \mathbf{N}_k^{\mathrm{T}}\,\overline{\mathbf{u}}\,d\Gamma.$$

The solution of the system of equations (9) is the vector $\mathbf{u}$, which is a vector of the nodal parameters of the displacements for the problem under consideration. The displacements at any field point, including the model nodes, can be obtained by equation (3).

2.4. Enrichment of EFG method for the crack tip vicinity

The EFG method is very efficient for fracture mechanics problems. The vicinity of the crack tip can be easily modelled by inserting additional nodes within this region, to capture the stress intensity with the desired accuracy. Furthermore the performance of the method seems to be minimally effected by irregular arrangement of the nodes [7].

Alternatively, in order the avoid large arrays of nodes at the crack tip, special techniques have been developed for modelling in detail the singular functions associated with elasto-static fracture. As a general rule for mesh-less methods, a sharp gradient in nodal spacing leads to error, because the nodes in the coarse region have domains of influence extended to the refined area, while-vice versa is not true. An incorporation of the singular fields in a mesh-less method is substantially simpler and more trouble-free than in the finite element method and does not require mesh refinement [11].

Enrichment of a mesh-less method could be achieved extrinsically or intrinsically. The former consists of adding an enrichment function to the trial function, which leads to the additional unknowns associated with crack tip (stress intensity factors). Contrary, the intrinsic enrichment involves no additional unknowns. In this technique, the entire near tip asymptotic displacement field is included in the basis.

In this paper, the capturing of $1/\sqrt{r}$ stress singularity in linear elastic fracture mechanics (LEFM) is achieved by using the following full intrinsic basis enrichment [11], [12], [13]:

$$\mathbf{p}^{\mathrm{T}}(\mathbf{x}) = \left[1, x, y, \sqrt{r}\cos\frac{\theta}{2}, \sqrt{r}\sin\frac{\theta}{2}, \sqrt{r}\sin\frac{\theta}{2}\sin\theta, \sqrt{r}\cos\frac{\theta}{2}\sin\theta\right], \tag{12}$$

where r and θ are polar coordinates for a coordinate system with an origin set at the crack tip. The linear terms in equation (12) are not related to the near tip fields.

It should be pointed out that because of the increased size of the basis, additional computational effort is required to invert the moment matrix $\mathbf{A}(\mathbf{x})$ from equation (4), in spite of the reduction of the nodes. Moreover, the domain of influence must be enlarged to achieve a regularity of $\mathbf{A}(\mathbf{x})$. The scaling parameter $d_{\max}$ controlling the size of the domain of influence is assumed equal from 3 to 3.5 in this paper, while without enrichment the same parameter can

be taken 2 or even 1.5.

The given below numerical simulations are achieved by using the full basis enrichment presented with equation (12). Without enrichment, the EFG method requires considerable nodal refinement near the crack tip to capture the stress singularity with sufficient accuracy. Contrary, the enriched EFG method is able to capture the singularity of the crack tip without using extra refinement at this region.

A MATLAB software code, for two dimensional elasticity problems, has been developed based on theory just described as well as on the MATLAB source programs given in paper [9]. Many numerical examples have been calculated as well as a set of standard patch tests. Comparisons have been made with exact analytical solutions by using both linear and quadratic basis functions. The quadratic basis gives more accurate results compared with a linear one in some cases of higher order patches with irregular node arrangements, for example the patch test of pure bending. The numerical simulations have shown better accuracy compared with finite element method by using a similar mesh.

3. Formulation of the fracture mechanics problem

The problem under consideration is a plane structure of thickness b in which a pre-existing crack of length a is available (Fig. 1). The crack propagates under pure opening mode I of fracture. The problem which is worked out in this paper is the determination of stress intensity factor,K_{I}, due to the prescribed external loads. It can be said that the derivation of the energy release rate is also developed bearing in mind the certain relationship between the energy release rate, $\mathcal{G}_{\mathrm{I}}$, and the SIF, namely $\mathcal{G}_{\mathrm{I}} = K_{\mathrm{I}}^2/E$ (E is the modulus of elasticity).

In linear elastic fracture mechanics, the nonlinearity, respectively fracture process, occurs at a single mathematical point at the crack tip [2]. That is way in the specimens under consideration always an initial crack must be available. The fracture process presented in a general force – general displacement plot ($F-u$ plot) is the usual way of plotting experimental results. Thus, with the numerical simulations, which are compared with experimental evidence, the aim is to derive the similar curve. Usually the general force, F, is the force parameter: P in Fig. 1(a) and 1(b); the intensity of the distributed load, q, in Fig. 1(c). The general displacement is the displacement or sum of displacements, which have a contribution to the work of external forces, respectively to the energy release. For the example shown in Fig. 1a, the typical displacement

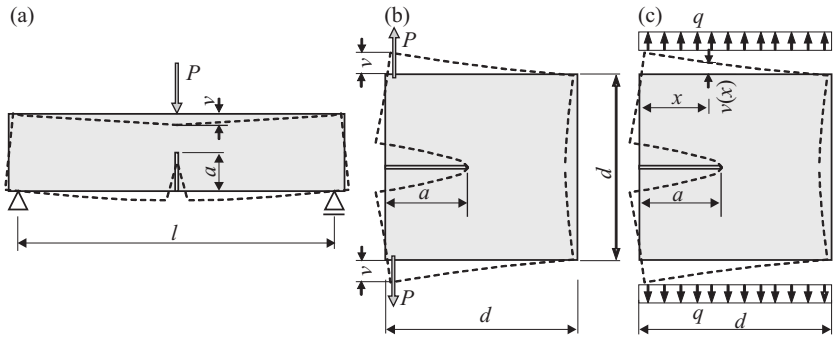

Fig. 1. Plane structures of thickness b with a pre-existing crack of length a

is $u = v$; in the case of Fig. 1(b) the typical displacement is mutual vertical deflection of the points of application of the forces, $u = 2v$. For the example shown in Fig. 1(c) the typical displacement is the integral of vertical displacements along upper and lower edges of the plane structure, or $u = 2\int_0^d v(x)dx$. The $F - u$ plots give the relationship between force and typical displacement, of the model under consideration, with crack growing. The crack grows statically under constant fracture energy G_f. The latter is called specific fracture energy, which is the work needed to separate two faces of a unit surface of the crack. G_f is a material parameter given from the experiment. In our case of prescribed external loads, the material parameters such as fracture energy, G_f, or fracture toughness,K_{Ic}, are not necessary, so it is assumed that any reference values of them are in hand. The typical force-displacement graphics derived by LEFM principles has the appearance given in Fig. 2. The peak point of the curve usually is followed by a negative slope for the iso-G_f curve, although sometimes certain geometry exists where this curve displays positive slope.

Each single point of the graphics in Fig. 2 corresponds to a different crack length. Points A_1 to A_{11} are derived for crack lengths a_1 to a_{11}. Let the shaded triangle OA_5A_6 is under consideration, at the point A_5 crack length is a_5. Along the line OA_5 energy release rate, $\mathcal{G}$, increases while the crack retains its initial value a_5. The crack grows under constant energy release rate $\mathcal{G} = G_f$ when the increasing energy release rate reaches the fracture energy, G_f. The line A_5A_6 corresponds to this stage. If at point A_6, where the crack length is a_6, the specimen is unloaded, the crack will not heal, so the unloading branch A_6O will take place at a constant crack length a_6 [2]. The derivation

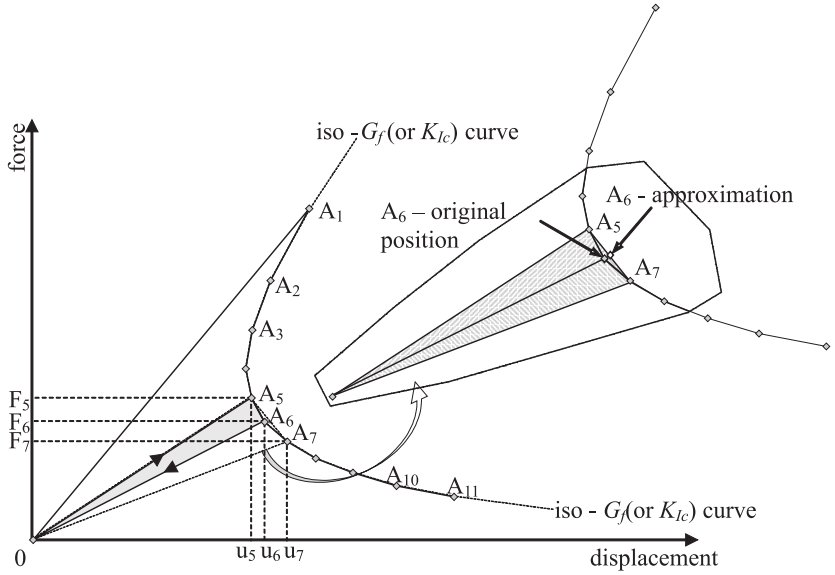

Fig. 2. Typical force-displacement curve obtained by LEFM principles

of linear LEFM curve requires previously accepted crack increment Δa, which usually remains constant during the fracture process. The area of the shaded triangle OA_5A_6 is the energy release available for fracture, for crack extension with length Δa [2]. This area must be equal to the energy required for crack extension with length Δa, respectively crack area is $\Delta a \cdot b$, the latter energy is $G_f \cdot \Delta a \cdot b$, where b is the specimen thickness.

3.1. Standard energy approach

The energy release rate is a state function. It depends on the instantaneous geometry and boundary conditions, but not on how they have been attained [2]. There are various numerical approaches for solving LEFM parameters. In this paper an idea related to a determination of energy release rate, based on the incremental stiffness method, is proposed. According to the standard application of this method the energy supplies for two close crack lengths should be derived (Fig. 3). The energy release rate is the limit of the area of any of the shaded triangles in Fig. 3 when the crack extension tends to zero [2]. Numerically, this statement is achieved by calculation of energy supply to the structure, respectively the work of external loads. The work of the external loads can be calculated for a given crack length and applied load (force, F, or displacement, u, in Fig. 3). The external work is $W_1 = Fu_1/2$ $(F = P)$ for the first example in Fig. 1(a), where u_1 is the displacement of the

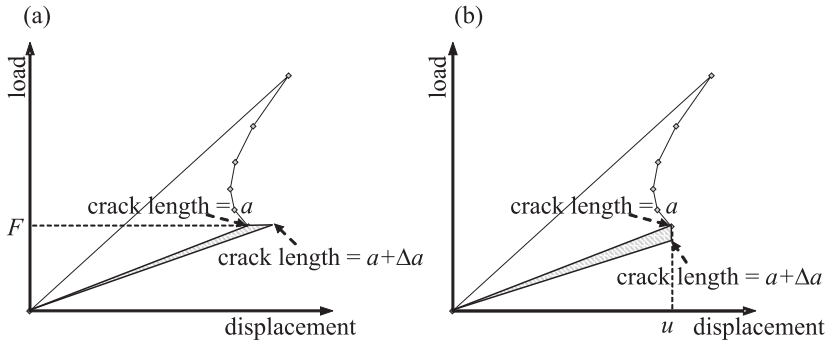

Fig. 3. Virtual incremental fracture process: (a) At constant load; (b) At constant displacement

point of application of the applied force, P, derived by the model with crack length equal to a. Then the infinitesimal crack increment, Δa, is introduced in the numerical model. The second external work is $W_2 = Fu_2/2$ for the same reference load and the new crack length, where u_2 is the vertical deflection of the point of application of the applied force for crack length equal to $a + \Delta a$. The difference between both the external works, $W_1 - W_2$ is the energy supplied for fracture, which must be equal to $\mathcal{G} \cdot b \cdot \Delta a$, respectively the required energy release rate, $\mathcal{G}$, can be obtained by the following expression:

$$\mathcal{G} = \frac{F(u_2 - u_1)}{2b\,\Delta a}. \tag{13}$$

The same procedure can be applied for two different and close crack lengths before, $a - \Delta a$, and after, $a + \Delta a$, the crack tip under consideration. Then, applying the aforementioned thoughts the energy release rate can be estimated as [2]:

$$\mathcal{G} = \frac{F^{ref}}{2} \frac{(u(a + \Delta a) - u(a - \Delta a))}{2\,b\,\Delta a}. \tag{14}$$

Finally, the necessary load level for fracture initiation can be derived by the condition that energy release rate for fracture mode I equals the fracture energy, G_f, for the same mode which is material parameter. The accuracy of the energy release rate in that case depends on the crack increment Δa. The smaller the crack increment, the more accurate results for energy release rate. Any commercial numerical method codes can be used for the presented method. Numerical resolution and mesh refinement limit the accuracy of the procedure.

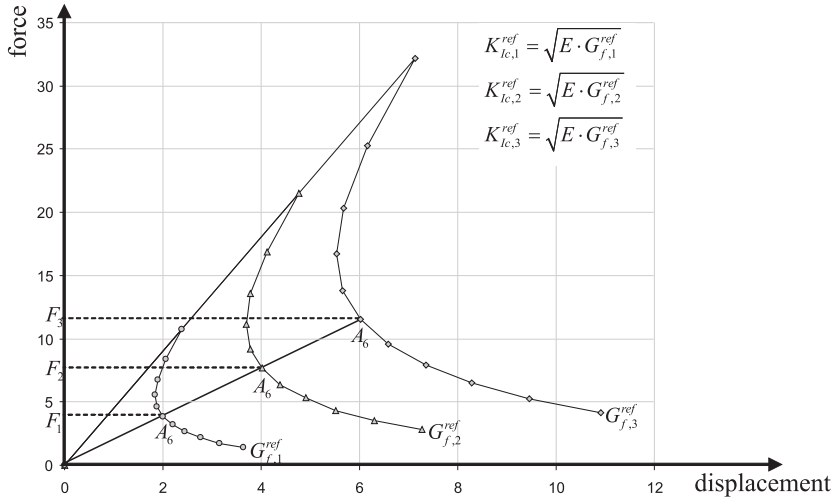

Fig. 4. Typical load-displacement curves obtained by LEFM for different values of fracture energy

3.2. Stress intensity factor calculation based on the standard appearance of the force-displacement curve

What follows is the explanation of one new idea related to the derivation of SIF based on the standard appearance of the force-displacement curve. It is well known, that the stress intensity factors are proportional to the applied external loads. Three different force-displacement curves are presented, for different fictitious reference values of the fracture energy G_f^{ref}, in Fig. 4. The critical SIF, called fracture toughness, K_{Ic}, corresponding to the reference values of the fracture energy, is $K_{Ic}^{ref} = \sqrt{E \cdot G_f^{ref}}$, bearing in mind the certain relationship between energy release rate and stress intensity factor. The forces $F_1 - F_3$ are the necessary loads for fracture initiation at the point A_6, calculated for the relevant material fracture toughness or fracture energy. If one of those curves is available, the SIF for a given external load, F, could be calculated using the following relations:

$$K_I = \frac{K_{Ic,1}^{ref}}{F_1} F = \frac{K_{Ic,2}^{ref}}{F_2} F = \frac{K_{Ic,3}^{ref}}{F_3} F, \tag{15}$$

which means that for calculation of SIF or energy release rate for a given external loads, a fictitious reference value of fracture toughness or fracture energy can be used.

Let us consider the point A_6 in Fig. 2. This point corresponds to a

crack tip with length a_6. Let us imagine that the whole graphics with points A_5, for the previous crack extension, and A_7, for the next crack increment, is available. The areas of both triangles OA_5A_6 and OA_6A_7 are equal to the energy supplied for fracture, for crack extension with lengthΔa. This area must be equal to $G_f^{ref} \cdot \Delta a \cdot b$, where G_f^{ref} is an arbitrary fictitious previously chosen reference value of the fracture energy.

If the crack extension Δa is small enough it could be assumed with sufficient accuracy that the three points A_5, A_6 and A_7 lie on a straight line. That straight line is a part of iso-G_f^{ref} curve, respectively iso-K_{Ic}^{ref} or iso-fracture toughness curve. The condition that the three points are placed on a straight line can be written as:

$$\begin{aligned} A\,u_5 + B &= F_5 \\ A\,u_6 + B &= F_6 \\ A\,u_7 + B &= F_7 \end{aligned} \quad . \tag{16}$$

In addition the equality of the shaded areas in Fig. 2 holds:

$$\begin{aligned} \frac{F_5 u_5}{2} - \frac{F_6 u_6}{2} + \frac{F_5 + F_6}{2}(u_6 - u_5) &= G_f^{ref} \cdot \Delta a \cdot b, \\ \frac{F_6 u_6}{2} - \frac{F_7 u_7}{2} + \frac{F_6 + F_7}{2}(u_7 - u_6) &= G_f^{ref} \cdot \Delta a \cdot b. \end{aligned} \tag{17}$$

A and B are unknown constants in equations (16). The forces F_5, F_6 and F_7 are unknown parameters as well as the displacements u_5, u_6 and u_7, but a certain relationship can be established between relevant forces and displacements. Three different static solutions should be performed in order to get such relation for the corresponding crack lengths – a_5, a_6 and a_7. Let the problem under consideration be the determination of SIF (or energy release rate) at the crack tip with length a_6 due to a given external force F. The displacements for the different crack lengths due to the applied loads obtained by linear elastic solutions are $\bar{u}_5$, $\bar{u}_6$ and $\bar{u}_7$. The forces corresponding to the actual values of displacements (Fig. 2) could be derived as:

$$F_5 = \frac{u_5}{\bar{u}_5} F;\ F_6 = \frac{u_6}{\bar{u}_6} F;\ F_7 = \frac{u_7}{\bar{u}_7} F. \tag{18}$$

In that case we have five unknown parameters: the constants A and B and the displacements u_5, u_6 and u_7. The solution of system of equations consists of expressions (16) and (17), accounting for relations (18), could be easily derived as follows:

$$u_5 = \sqrt{\frac{C_1 C_3}{C_2}},\ u_6 = \sqrt{\frac{C_1 C_2}{C_3}},\ u_7 = \sqrt{\frac{C_2 C_3}{C_1}}, \tag{19}$$

where C_1, C_2 and C_3 are constants defined as:

$$C_1 = \frac{2G_f^{ref} \cdot \Delta a \cdot b}{\frac{F}{\bar{u}_5} - \frac{F}{\bar{u}_6}},\ C_2 = \frac{2G_f^{ref} \cdot \Delta a \cdot b}{\frac{F}{\bar{u}_6} - \frac{F}{\bar{u}_7}} \text{ and } C_3 = \frac{4G_f^{ref} \cdot \Delta a \cdot b}{\frac{F}{\bar{u}_5} - \frac{F}{\bar{u}_7}}. \tag{20}$$

In that way, a real part $A_5A_6A_7$ from the force-displacement curve, for the fictitious value of fracture energy, assumed in advance, is reached. Having this part of the graphics available, taking into account equations (15), the stress intensity factor at point A_6 could be obtained as:

$$K_I = \frac{K_{Ic}^{ref}}{F_6} F, \tag{21}$$

respectively the energy release rate at that point is:

$$\mathcal{G}_{\mathrm{I}} = K_{\mathrm{I}}^2 / E. \tag{22}$$

It could be concluded that the problem solved, by the relevant approach, is the derivative of a function looking back at the aforementioned standard methodology for determination of the energy release rate. That is why the accuracy of the results depends on the increment Δa, which must be as small as necessary to calculate numerically the derivative of the energy release. In other words, the increment must gravitate to the point under consideration. Contrary, the methodology proposed in this paper is based on the standard appearance of the force-displacement curves. This approach catches the shape of the latter graphics around the point under consideration. In order to do that, the crack increment Δa must be chosen as small as necessary to draw the force displacement curve. If it is assumed that ten points are enough to get satisfactorily the curve from Fig. 2, then the crack increment could be set equal to 1/10 of the whole crack path. The latter means that the crack increment for the technique proposed here could be equal to the chosen crack length extension for determination of the crack path. This statement simplifies considerably the problem of crack propagation, because in order to calculate the stress intensity factors at the crack tip under consideration only one additional solution should be performed for the next tip, the previous one is currently available. The next solution will be useful for the coming (subsequent) crack tip and the following crack propagation. Contrary in the standard methodology, each single point of the force-displacement curve should be considered independently of the others. Moreover, in order to get energy release rate with sufficient accuracy the crack increment must be about 1/10 of the chosen crack length extension for crack propagation.

5. Numerical example

The presented numerical example is a square plate with an edge-crack of different length as shown in Fig. 1(c). The aim of these numerical simulations is to compare the SIFs obtained by the presented procedure with the analytical solutions given in [14]. In the EFG model twofold symmetry is taken into account to reduce the problem. Several nodes arrangements are used around the crack tip, in dependence on the crack lengths. A 10×5 array of cells is used along with 4×4 Gauss quadrature in all cells except those in the crack tip area where the Gauss points are 8×8. The numerical models for crack lengths $a = 0.4$; 0.45 and 0.425 are shown in Fig. 5.

In the MATLAB code intrinsic basis enrichment is incorporated in order to capture the stress singularity around the crack tip. So, in this case, additional nodes in the vicinity of the singular point are not necessary. In the numerical models from Fig. 5 however, extra nodes are introduced in order to take into account properly the boundary conditions for different crack lengths.

The normalized SIFs, $K_{\mathrm{I}}/(\sigma\sqrt{\pi a})$, for pure mode I of fracture, for various crack lengths are computed applying the presented procedure. The smallest crack length is 0.2, the largest one is 0.6. It is assumed that the crack grows from initial length of 0.2 to the final one of 0.8. The relevant crack length increment is 0.06 if the typical force-displacement curve consists of 10 subintervals. In that respect, two different crack length increments are considered for comparison and summary of the accuracy of the presented methodology. The first crack extension is chosen to be 0.05, the second one is twice smaller than the former of length 0.025.

The obtained normalized SIFs for each one of the crack lengths, $K_{\mathrm{I}}/\left(\sigma\sqrt{\pi a}\right)$, for both crack increments are presented in columns 2 and 4 in Table 1. The corresponding reference SIFs are given in column 6 of the same table. In all examples, the differences are given in columns 3 and 5, defined (%)

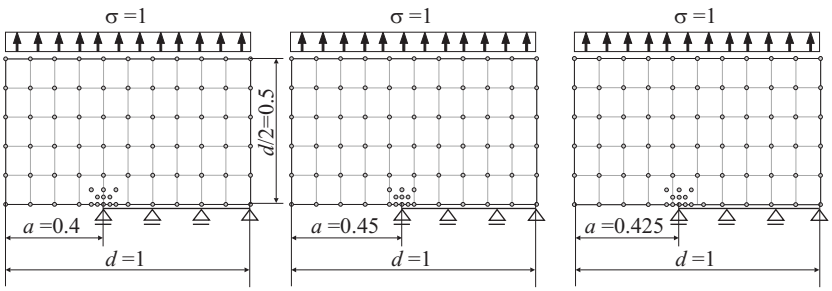

Fig. 5. EFG numerical models for different crack lengths

as – difference=$\left|K_I - K_I^{ref}\right| / K_I^{ref} \cdot 100$. For all numerical examples, except for the first crack length of $a = 0.2$ and increment $\Delta a = 0.05$, the error is less than 1% and decreases with decreasing of the crack increment. The obtained results are sufficiently accurate although the mesh is relatively coarse, and the crack extension is relatively large.

Table 1. SIF $K_{\mathrm{I}}^2/(\sigma\sqrt{\pi a})$, and difference relative to [14] for a plate with central crack

	$K_{\mathrm{I}}/(\sigma\sqrt{\pi a})$	Difference	$K_{\mathrm{I}}/(\sigma\sqrt{\pi a})$	Difference	$K_{\mathrm{I}}^{ref}/(\sigma\sqrt{\pi a})$
Crack length $a =$	Crack increment $\Delta a = 0.05$	%	Crack increment $\Delta a = 0.025$	%	Reference [14]
1	2	3	4	5	6
0.2	1.468	1.32	1.480	0.52	1.488
0.3	1.831	0.90	1.840	0.45	1.848
0.4	2.308	0.69	2.313	0.47	2.324
0.5	2.990	0.66	2.994	0.52	3.010
0.6	4.111	0.98	4.120	0.76	4.152

In case of necessity, the accuracy of the SIFs could be improved by refinement of the model mesh. The normalized SIFs for crack length increment equal to 0.025 and refined model mesh are plotted in column 3 of the Table 2. The mesh is regular of a 40×20 array of cells without additional nodes around the crack tip. The accuracy of the SIF is improved at the expense of the refined model mesh and respectively the computational time.

Table 2. SIF $K_{\mathrm{I}}^2/(\sigma\sqrt{\pi a})$ obtained with the refined model mesh

	$K_{\mathrm{I}}/(\sigma\sqrt{\pi a})$	Difference	$K_{\mathrm{I}}^{ref}/(\sigma\sqrt{\pi a})$
Crack length $a =$	Crack increment $\Delta a = 0.025$	%	Reference [14]
1	2	3	4
0.2	1.483	0.36	1.488
0.3	1.845	0.19	1.848
0.4	2.321	0.14	2.324
0.5	3.006	0.12	3.010
0.6	4.144	0.18	4.152

Based on the above numerical example and comparison of the results it could be concluded that the presented procedure for calculation of mode I stress intensity factors works with sufficient accuracy.

6. Conclusion

The aim of this paper is to provide one simple and reliable method for relatively accurate calculation of mode I stress intensity factors in LEFM. That method is based on the general shape of force-displacement curve. In fact, at first the shape of the curve around the current crack tip is reached and then having the graphics available, indirectly the SIF, respectively energy release rate, are obtained. There are plenty of different and quite accurate procedures for SIF calculations, which are available now in the literature. One advantage of the method proposed here is that it is applicable for all numerical methods and could be developed by any general purpose software program. That method is reliable with relatively coarse model mesh and could be used with relatively large crack increments. In fact, the latter could be equal to the chosen crack increment for determination of the crack path, which gets together the problems of crack propagation and SIF determination.

A MATLAB code, based on the element free Galerkin method for two dimensional elasticity problems is developed along with the presented procedure. The meshless methods, in particular EFG method, seams to be very appropriate for fracture mechanics problems because a progressively crack growing can be easily modelled by moving the fine node arrangement around the crack tip vicinity throughout the rest of the regular mesh. Also, the intrinsic basis enrichment is involved in the MATLAB code for modelling of the singular stress field around the crack tip. The latter enrichment requires substantially greater running time, because of the larger basis, but at the expense of the coarse mesh and more accurate results.

The procedure presented in this paper could be extended for the case of mixed mode of fracture by using appropriate decomposition of the energy release. A procedure for crack propagation could be developed having a reliable and simple method for SIF calculation for both opening and shearing fracture modes. At first, in the MATLAB code should be implemented a technique for internal crack modelling, because the domain of influence for a node near to the one side of the crack, should not affect the points to the other crack face. The latter will be an objective of the future work.

As a final conclusion it could be state that very accurate results for mode I stress intensity factors can be obtained by applying the method presented here.

REFERENCES

[1] Anderson, T. L. Fracture Mechanics Fundamentals and Application, Boca Raton, FL: CRC Press, 1991.

[2] Bazant, Z., J. Planas. Fracture and Size Effect in Concrete and Other Quasibrittle Materials, CRC Press, LLC, 1998.

[3] Williams, M. L. Stress Singularities Resulting from Various Boundary Conditions in Angular Corners of Plates in Extension. *J. Appl. Mech. ASME*, **19** (1952), 526–528.

[4] Bank-Sills, L., D. Ashkenazi. A Note on Fracture Criteria for Interface Fracture. *International Journal of Fracture*, **103** (2000), 177–188.

[5] Lankaster, P., K. Salkauskas. Surfaces Generated by Moving Least Squares Methods. *Mathematics of computation*, **37** (1981), No. 155, 141–158.

[6] Nayroles, B., G. Touzot, P. Villon. Generalizing the Finite Element Method: Diffuse Approximation and Diffuse Elements. *Computational Mechanics*, **10** (1992), 307–318

[7] Belytschko, T., Y. Y. Lu, L. Gu. Element Free Galerkin Methods. *International Journal of Numerical Methods in Engineering*, **37** (1994), 229–256.

[8] Belytschko, T., Y. Krongauz, D. Organ, M. Fleming, P. Krysl. Meshless Methods: An Overview and Recent Developments. *Computer Methods in Applied Mechanics and Engineering*, **139** (1996), 3–47.

[9] Dolbow, J., T. Belytschko. An Introduction to Programming the Meshless Element Free Galerkin Method. *Archives of Computational Methods in Engineering* (State of the art reviews), **5** (1998), 207–241.

[10] Liu, G. R., Y. T. Gu. Introduction to Meshfree Methods and Their Programming, Dordrecht, Springer, 2005.

[11] Belytschko, T., Y. Y. Lu, L. Gu. Crack Propagation by Element-free Galerkin Methods. *Engineering Fracture Mechanics*, **51** (1995), No. 2, 295–315.

[12] Rao, B. N., S. Rahman. An Efficient Meshless Method for Fracture Analysis of Cracks. *Computational mechanics*, **26** (2000), 398–408.

[13] Rao, B. N., S. Rahman. A Coupled Meshless-Finite Element Method for Fracture Analysis of Cracks. *International Journal of Pressure Vessesls and Piping*, **78** (2001), 647–657.

[14] Tada, H., P. C. Paris, G. R. Irwin. The Stress Analysis of Cracks Handbook, PA, Hellertown, Del Research Corporation, 1973.